Nanosecond Fluorescence Anisotropy Decays of *n*-(9-Anthroyloxy) Fatty Acids in Dipalmitoylphosphatidylcholine Vesicles with Regard to Isotropic Solvents†

Michel Vincent, Béatrice de Foresta, Jacques Gallay, and Annette Alfsen*

ABSTRACT: A set of *n*-(9-anthroyloxy) fatty acids [2-, 7-, 9-, and 12-(9-anthroyloxy)stearic acid (AS) and 16-(9-anthroyloxy)palmitic acid (16-AP)] has been studied by time-resolved and steady-state fluorescence anisotropy measurements in isotropic media (i.e., propylene glycol and a liquid paraffinic oil, Primol 342) and in vesicles of dipalmitoylphosphatidylcholine. The two modes of rotation, "in-plane" and "out-of-plane", of the anthroyl ring can be detected by varying the excitation wavelength. In both isotropic solvents, the value of the in-plane rotational rate is of the same order of magnitude as the out-of-plane rate for each one of the *n*-(9-anthroyloxy) fatty acids. In propylene glycol, the anthroyl ring motions are similar for all derivatives except for the 16-AP for which the fluorophore rotates at a higher rate. In the liquid paraffinic oil, identical motions of the fluorophore are observed for the 7-, 9-, and 12-AS; the motion for the 16-AP is again faster, while that for the 2-AS is slower. Moreover, the fluorophore motion for each probe is faster in this solvent than in propylene glycol in conditions of identical viscosity. When embedded in phospholipid bilayers, these probes report the microenvironment at a graded series of depths from the surface to the center of the bilayer [Haigh, E. A., Thulborn, K. R., & Sawyer, W. H. (1979) *Biochemistry 18*, 3525-3532]. Studies in dipalmitoylphosphatidylcholine vesicles have been performed at three temperatures (21, 37, and 47 °C) corresponding to different lipid phases. The out-of-plane mode of rotation is unhindered as demonstrated by an anisotropy decay profile asymptotic to zero. Thus, evaluation of a membrane "fluidity" parameter at different depths of the bilayer is possible, even in the steady-state mode of observation. When the in-plane mode of rotation contributes to the anisotropy decay, a hindrance to the motion is observed below the gel to liquid-crystalline transition. Then information about lipid order can be obtained from the plateau value (r_∞) of the fluorescence anisotropy decay. In the pretransition temperature range (37 °C), the results evidence the existence of structural lipid changes mainly localized in the hydrophobic core of the bilayer. The main transition leads to a complete disappearance of the hindrances on the in-plane rotation.

Fluorescence techniques have provided useful information about lipid organization and dynamics in both model and biological membranes (Vanderkooi & McLaughlin, 1975). In particular, fluorescence anisotropy measurements are related to the rotational motion of the probe, reflecting the frictional retardation forces imposed by its microenvironment (Perrin, 1936; Weber, 1953). These measurements have been widely used for the estimation of the membrane "fluidity" (Shinitzky & Barenholz, 1978). The validity of this parameter has yet been questioned (Hare et al., 1979), and some conditions relative to its obtention will be discussed below.

The uncertainty about the location of some probes in membrane systems, pointed out by Lentz et al. (1976) and Lakowicz & Knutson (1980), is one of the difficulties that can lead to some misinterpretations of the data. Due to their structural analogy with the membrane lipid components, the *n*-(9-anthroyloxy) fatty acids are likely to fit in the membrane with their acyl chains parallel to those of the phospholipids. These probes allow a labeling at a graded series of depths in the bilayer, as demonstrated by fluorescence quenching and energy transfer experiments (Thulborn & Sawyer, 1978; Haigh et al., 1979). Consequently, they have been used in order to estimate membrane fluidity gradients (Tilley et al., 1979; de Paillerets et al., 1981). However, even in an isotropic medium, differences are expected in the intrinsic fluorescence and motional properties of the anthroyl ring as a function of its position of substitution on the acyl chain. Such differences in motional behavior have been hinted by steady-state fluorescence polarization measurements at one excitation wavelength (Tilley et al., 1979), and they have to be taken into account for the interpretation of the data obtained in membranes. Furthermore, the motion of this disklike fluorophore is the result of at least two principal modes of rotation: "in-plane" and "out-of-plane". For the evaluation of each rate, steady-state and dynamic fluorescence depolarization measurements have to be performed at different excitation wavelengths, corresponding to different angles between absorption and emission oscillators (Weber, 1971).

Another difficulty in the determination of membrane fluidity is the existence of hindered rotational motions of fluorescent probes, which has been stated for rod- as well as for disklike probes [respectively diphenylhexatriene (Kawato et al., 1977; Lakowicz et al., 1979) and parinaric acid (Wolber & Hudson, 1981) and perylene (Lakowicz & Knutson, 1980), 8-anilino-1-naphthalenesulfonic acid (Kinosita et al., 1976; Wahl et al., 1971), and 2-anilinonaphthalene (Badea et al., 1978)]. Such hindered motion is evidenced on the anisotropy decay curve by the persistence of a nonzero value of the fluorescence anisotropy at long times as compared to the excited-state lifetime of the probe. This nonzero value has been interpreted either in terms of reflecting barriers, within the framework of the model first proposed by Wahl (1975a,b) and further extended to a cone model by Kinosita et al. (1977), or in terms of an orientational distribution function (Heyn, 1979; Lipari & Szabo, 1980).

In the first part of this work, steady-state and time-resolved fluorescence anisotropy measurements were carried out in order to determine the motional properties of the *n*-(9-

† From Equipe de Recherche No. 64 du Centre National de la Recherche Scientifique and Unité 221 de l'Institut National de la Santé et de la Recherche Médicale, Unité d'Enseignement et de Recherche Biomédicale des Saints-Pères, Université Paris V, 75006 Paris, France. *Received April 8, 1981; revised manuscript received August 7, 1981.* This work was supported in part by Grant CRL 813035 from INSERM.

* Address correspondence to this author at the Etats Lies Moleculaires, 45 rue des Saints-Pères, 75270 Cédex 06 Paris, France.

0006-2960/82/0421-0708$01.25/0

anthroyloxy) fatty acids in two isotropic media: a liquid paraffinic oil (Primol 342) and propylene glycol. The differences in the rotational rates observed in these two media are discussed in relation to solvation effect, bulk viscosity, and substitution position of the anthroyl ring on the acyl chain. In the second part, these probes were used to describe the structural organization of DPPC[1] vesicles at different temperatures. The evaluation of hindrances imposed on each type of rotational motion of the fluorophore would be expected to bring more insight on the anisotropy of the membrane structure.

Materials and Methods

Chemicals. Primol 342 was a gift of ESSO Research Laboratory (Mont St. Aignan, France) and was free of fluorescent impurities. Propylene glycol was from Merck (Darmstadt, Germany) and used as supplied. Dipalmitoylphosphatidylcholine (DPPC) (Serdary, Canada) was used as purchased. This chemical migrated as a single spot on silica with chloroform–methanol–water (65:25:5 v/v/v) as solvent. *n*-(9-Anthroyloxy) fatty acids were from Molecular Probes (Plano, CA). Their purity was controlled by thin-layer chromatography with ethanol–water (95:5 v/v) as solvent (Vanderkooi et al., 1974). All other reagents were of the highest grade commercially available.

Phospholipid Samples. Ethanol-injected vesicles were prepared from 20 mg/mL ethanolic solutions of DPPC by the method of Kremer et al. (1977). The injection of 600 μL of DPPC ethanolic solution in 20 mL of 0.05 M Tris-HCl and 0.1 M NaCl, pH 8, buffer was performed above the transition temperature. The sample was passed through a 450-nm Millipore filter. Lipid vesicles were labeled by adding 3 μL of a 1 mg/mL tetrahydrofuran solution of *n*-(9-anthroyloxy) fatty acids in 3 mL of buffer containing the vesicles (probe:phospholipid molar ratio $\simeq$ 1:400). One blank was performed by adding the same tetrahydrofuran aliquot without fluorescent probe to the lipid vesicle suspension.

Absorption Measurements. They were carried out on a Cary 118 spectrophotometer.

Viscosity Measurements. Viscosity values of Primol 342 were measured with a FICA viscosimatic M-S apparatus equipped with an Ubbelhode viscosimeter (1.83-mm diameter) and thermostated with a Huber HS 60 apparatus (Öffenburg, Germany). Calibration was performed with propylene glycol. Densities were measured with a PAAR DMA 40 densitometer.

Steady-State Fluorescence Measurements. The steady-state fluorescence emission anisotropies were measured with a T-format SLM 8000 photon counting spectrofluorometer (Urbana, IL) equipped with a single grating excitation monochromator (MC 320) and Glan Thompson polarizers. The sample cell holder was regulated by a Huber HS 60 thermostat. Temperature in the sample was checked by means of a digital thermometer Digitec 5810 (Dayton, OH) with a YSI thermocouple (Yellows Springs, OH). For the polarization excitation spectra, the band-pass was set to 1 nm, and fluorescence emission was collected through Schott KV 418 cutoff filters. The emission anisotropies were calculated according to

$$r = \frac{R(\text{vert}) - R(\text{horz})}{R(\text{vert}) + 2R(\text{horz})}$$

where $R(\text{vert}) = I_{vv}/I_{vh}$ and $R(\text{horz}) = I_{hv}/I_{hh}$, the first and the second subscripts referring to excitation and emission components, respectively. These relative intensities were directly recorded with the ratio mode in order to eliminate source intensity fluctuations. $R(\text{horz})$ is a calibration factor, which normalizes the output response of each analysis channel. When necessary, the contribution of scattering or solvent background to the fluorescence intensity can be automatically subtracted on each channel, leading to the corrected new ratios:

$$R(\text{vert}) = \frac{I_{vv} - I'_{vv}}{I_{vh} - I'_{vh}} \qquad R(\text{horz}) = \frac{I_{hv} - I'_{hv}}{I_{hh} - I'_{hh}}$$

where the prime refers to the blank.

Steady-State Data Analysis. The results were interpreted according to the formalism developed by Weber (1971) and Shinitzky et al. (1971). These authors have derived an approximate form for the relation between the anisotropy values of fluorescent rotating plates and their rates of rotation, in the case where absorption and emission oscillators are coplanar and where only small rotations can take place between excitation and emission:

$$r_0/r = 1 + 6\tau\left(\frac{R_{ip}(2\cos^2\alpha - 1) + R_{op}\cos^2\alpha}{3\cos^2\alpha - 1}\right) \quad (1)$$

where τ is the excited state lifetime, α is the angle between the absorption and emission oscillators, R_{op} is the rate of rotation about an axis perpendicular to the absorption oscillator and contained in the ring plane, i.e., an out-of-plane rate of rotation, and R_{ip} is the rate of rotation about an axis normal to the ring plane, i.e., an in-plane rate of rotation. Since the direction of the absorption oscillator may change as a function of the excitation wavelength, as reflected by the r_0 values, the R_{op} values may not correspond to the same rotation of the molecule when excited at different wavelengths, as stressed by Weber (1971).

The quantity $[(r_0/r) - 1]/\tau$, which according to eq 1 is proportional to an average rate of rotation of the fluorophore, has been plotted as a function of excitation wavelength. Variation of this quantity would indicate anisotropic motion of the fluorophore (Shinitzky et al., 1971; Valeur & Weber, 1978).

The determination of R_{ip} and R_{op} has been performed according to a graphic method. By replacing $\cos^2\alpha$ by its expression in function of r_0:

$$\cos^2\alpha = (5r_0 + 1)/3$$

eq 1 becomes

$$Y = R_{ip}X + R_{op} \quad (2)$$

with

$$Y = \frac{5r_0}{2\tau}([(r_0/r) - 1]/(5r_0 + 1))$$

and

$$X = (10r_0 - 1)/(5r_0 + 1)$$

Y and X have been calculated from the r_0 and r experimental values at each wavelength in the 300–400 nm range, and Y has been plotted as a function of X. If the curve is fitted by a straight line, this should indicate that R_{op} is constant. Then, the slope of this straight line and its intercept with the ordinate axis yield R_{ip} and R_{op}, respectively. Error bars ΔX and ΔY have been calculated taking $\Delta r = \Delta r_0 = 0.002$ and neglecting errors on τ.

Nanosecond Anisotropy Decay Measurements. The time courses of the emission anisotropy were obtained with a single

[1] Abbreviations: DPPC, dipalmitoylphosphatidylcholine; *n*-AS, *n*-(9-anthroyloxy)stearic acid; 16-AP, 16-(9-anthroyloxy)palmitic acid; DPH, 1,6-diphenyl-1,3,5-hexatriene; Tris, tris(hydroxymethyl)aminomethane; ^{13}C NMR, carbon-13 nuclear magnetic resonance.

photon counting fluorometer (Applied Photophysics, system SP7 and Ortec system 9200 electronic device), as previously described (Gallay et al., 1981; de Paillerets et al., 1981). Excitation wavelength was selected by a grating monochromator. Emission light was collected through a cutoff filter Schott KV 418. Polaroid films were used on excitation and emission sides. The flash lamp was filled with air, under a pressure of 0.5 atm. In these conditions, spectral lines are normally obtained with the strongest lines centered at 316, 337, 358, and 381 nm. The emission decay curves $I_{vv}(t)$ and $I_{vh}(t)$ of the sample, from which a blank was subtracted when needed, were collected successively for time periods in the range of 5–20 min, depending on sample intensity. The experimental sum $s(t)$ and difference $d(t)$ decays were calculated from the data according to

$$s(t) = [I_{vv}(t)]G + 2I_{vh}(t)$$
$$d(t) = [I_{vv}(t)]G - I_{vh}(t)$$

where G is a correction factor for the fluctuations in excitation intensity and for the difference in the response of the analysis photomultiplier to differently polarized light; G is given by

$$G = [(1 + 2r)/(1 - r)][\sum I_{vh}(t)/\sum I_{vv}(t)]$$

where r is the steady-state anisotropy of the sample determined as described above and $\sum$ refers to the summation of the counts for each curve over all the analyzer channels (Dale et al., 1977).

The impulse responses $S(t)$ and $D(t)$ are related to the experimental functions $s(t)$ and $d(t)$ by the convolution integrals:

$$s(t) = \int_0^t S(t - t')g(t')\,dt'$$

and

$$d(t) = \int_0^t D(t - t')g(t')\,dt'$$

A mono- or biexponential decay is assumed for $S(t)$ and $D(t)$, the parameters of which are computed using the modulation function method according to Valeur (1978), followed for $S(t)$ by a nonlinear least-squares regression. A first approximation of the parameters of $r(t)$, also assumed to be mono- or biexponential, is given by calculating the ratio $D(t)/S'(t)$, where $S'(t)$ is equal to $S(t)$ when this last function is monoexponential. When it is not the case, $S'(t)$ is chosen as

$$S'(t) = a' \exp(-t/\tau')$$

where τ' is the mean excited state lifetime calculated as $(\sum_i a_i\tau_i^2)/(\sum_i a_i\tau_i)$ and a' as $\sum_i a_i$ (Chen et al., 1977). Starting from these calculated parameters of $r(t)$, a nonlinear least-squares regression is performed, fitting the convolution product of $g(t)$ and $r(t)S(t)$ to the experimental curve $d(t)$, in which the parameters of $S(t)$ are held constant and only those of the emission anisotropy decay are adjusted. When one of the decay-time components of $r(t)$ is long as compared to the mean lifetime of the excited state, a nonexponential function of the form

$$r(t) = r_1 \exp(-t/\Phi) + r_\infty$$

can be used as a trial function for the analysis. r_1 can be written as

$$r_1 = r_{t=0} - r_\infty$$

where $r_{t=0}$ is the anisotropy at zero time. In this case, Φ has been interpreted in terms of a relaxation time with which the equilibrium distribution of the probe excited state inside a cone is approached (Kinosita et al., 1977).

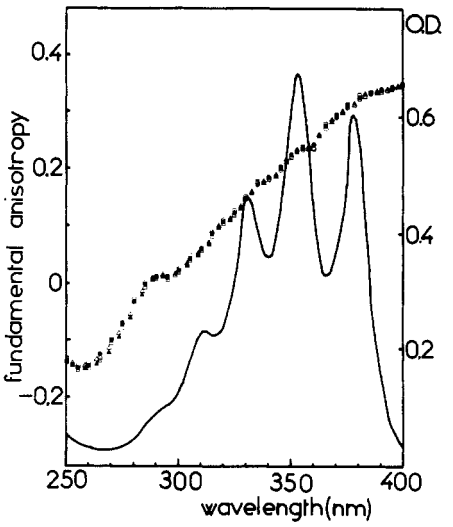

FIGURE 1: Fundamental anisotropy spectra of 2-AS (▲), 7-AS (○), 9-AS (●), 12-AS (△), and 16-AP (□) in propylene glycol at −52 °C. Absorption spectrum of 9-AS (–) in the same medium at room temperature. Probe concentration 7×10^{-5} M.

Perrin Plots. Values of $1/r$ have been plotted as a function of $(T\tau)/\eta$, according to Perrin (1926), where T is the absolute temperature, τ the excited state lifetime, and η the solvent viscosity. Extrapolation at $(T\tau)/\eta = 0$ leads to the value of r_0^{-1}.

Results

Fluorescence Properties of n-(9-Anthroyloxy) Fatty Acids in Propylene Glycol. In the general case of completely asymmetric fluorophores, the steady-state fluorescence anisotropy is related by a complex function to the rotational rates of the molecule (Weber, 1971). For planar aromatic molecules, the steady-state measurements can yield an average rate of rotation simply expressed as a function of the in-plane and out-of-plane rates of rotation and of the fundamental anisotropy value (r_0). The in-plane (R_{ip}) and the out-of-plane (R_{op}) rates are expected to be measured for r_0 values equal to −0.2 ($\alpha = 90°$) and 0.1 ($\alpha = 45°$), respectively, while they are equally weighted for r_0 equal to 0.4 ($\alpha = 0°$) (Weber, 1971; Shinitzky et al., 1971; Valeur & Weber, 1978).

The fundamental anisotropy spectra (r_0 vs. excitation wavelength, measured in propylene glycol at −52 °C) of the *n*-(9-anthroyloxy) fatty acids appear to be identical, whatever the substitution position (Figure 1). The value of $r_0 = 0.1$ is obtained at 319 nm, but the 0.4 and −1/5 values are never reached in the wavelength range studied. The anisotropy values (r) of this set of probes were measured as a function of excitation wavelength, in the same medium at −10 °C. At this temperature the viscosity of the solvent (490 cP) is in the range of the viscosities usually ascribed to membranes (Shinitzky & Barenholz, 1978), though the limits of validity of this parameter for such systems are already known (Kinosita et al., 1977; Hare et al., 1979). Excited-state lifetimes (τ) were measured for all probes at the same temperature (−10 °C). The total intensity decay curves were best fitted with a single exponential, and lifetime values (± 0.2 ns) are 11.3, 10.6, 10.4, 10.6, and 10.4 ns for 2-, 7-, 9-, and 12-AS and 16-AP, respectively. The plots of $[(r_0/r) - 1]/\tau$ vs. excitation wavelength are given in Figure 2. For all curves, no significant deviation from the horizontal is observed (Figure 2), which is an indication of isotropic motion of the fluorophore, whatever the substitution position. The values of $[(r_0/r) - 1]/\tau$ allow a comparison between the average rotational rates of the dif-

Table I: Computed Out-of-Plane (R_{op}) and In-Plane (R_{ip}) Rotational Rates and Corresponding Rotational Correlation Times[a] (ϕ_{op} and ϕ_{ip}) of *n*-(9-Anthroyloxy) Fatty Acids in Propylene Glycol at −10 °C

probe[b]	R_{op} (MHz)	ϕ_{op} (ns)	R_{ip} (MHz)	ϕ_{ip} (ns)
2-AS	3.5	48	3.5	48
7-AS	4.1	41	5.1	33
9-AS	4.6	36	5.0	33
12-AS	4.6	36	5.5	30
16-AP	8.6	19	9.1	18

[a] Calculated as $\phi_{op} = 1/(6R_{op})$ and $\phi_{ip} = 1/(6R_{ip})$ according to Yguerabide et al. (1970). [b] Probe concentration 7×10^{-5} M.

Table II: Rotational Correlation Time Values (ns)[a] of the *n*-(9-Anthroyloxy) Fatty Acids in Propylene Glycol at −10 °C

	excitation wavelength[c]	
probe[b]	316 nm	381 nm
2-AS	27	35
7-AS	25	33
9-AS	25	32
12-AS	26	30
16-AS	15	17

[a] ±1 ns. [b] Probe concentration 1.5×10^{-5} M. [c] Band-pass 10 and 2 nm for 316 and 381 nm, respectively.

ferent probes; these average rates are quite similar for the 2-, 7-, 9-, and 12-AS probes but significantly lower than the average rate of the 16-AP. For determination of the R_{ip} and R_{op} values, the anisotropy values have been plotted according to eq 2, as described under Materials and Methods. As an example, this plot is given for 9-AS (Figure 3). For all probes the points are well fitted to a straight line (correlation coefficients ≥ 0.958). Therefore, it has been possible to compute the values of R_{ip} and R_{op} (Table I). The values obtained show that the condition of validity of the plots ($R \times \tau$ is small compared to unity) is fulfilled since $R \times \tau < 0.1$ for the most rapid probe (16-AP). No significant difference between these two rates of rotation is obtained for each probe, taking into account the precision of the determination of R_{ip} and R_{op}. The comparison of the results obtained for the different probes evidences a slight increase in the rotational rates from the 2-AS to the 12-AS, both rates being twice as high for the 16-AP (Table I).

Time-resolved measurements have also been performed at −10 °C. Two excitation wavelengths have been selected, taking into account the fundamental anisotropy values and the lamp spectral lines. At 316 nm, where r_0 is nearly equal to 0.1, a valuable estimation of the out-of-plane mode of rotation is expected. When the excitation wavelength is set at 381 nm ($r_0 = 0.324$), the two modes of rotation contribute about equally to the depolarization (Kinosita et al., 1977). All experimental anisotropy decay curves were best fitted with a

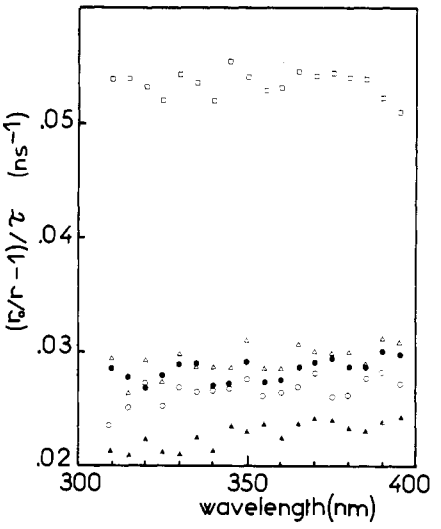

FIGURE 2: Plots of $[(r_0/r) - 1]/\tau$ vs. excitation wavelength in propylene glycol at −10 °C for 2-AS (▲), 7-AS (○), 9-AS (●), 12-AS (△), and 16-AP (□). Probe concentration 7×10^{-5} M.

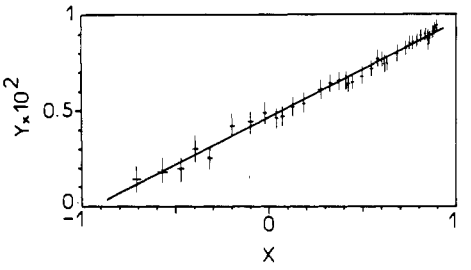

FIGURE 3: Plot of $Y = f(X)$ for the 9-AS in propylene glycol. Y and X parameters are described under Materials and Methods.

single exponential. The results obtained are presented in Table II. For each probe, the value of correlation time is slightly different at the two excitation wavelengths. No significant difference in the rotational motion properties occurs between the 2-, 7-, 9-, and 12-AS probes, while the motion of the 16-AP is 2 times faster. The coincidence, within the experimental error, between the r_0 values measured in vitrified propylene glycol and the anisotropy at zero time ($r_{t=0}$) obtained from the decay curves at both excitation wavelengths is to be emphasized (Table III).

Fluorescence Properties of n-(9-Anthroyloxy) Fatty Acids in Primol 342. For evaluation of the rotational motion properties of this set of probes in a hydrophobic medium, similar experiments were performed in a liquid paraffinic oil, i.e., Primol 342, whose viscosity temperature dependence is similar to the one of the widely used White American Oil USP 35 (Hare & Lussan, 1977). The anisotropy spectra at 6 °C of these probes are presented in Figure 4. At this temperature the viscosity value of Primol is equal to 510 cP. The same anisotropy values are obtained for the 2-, 7-, 9-, and 12-AS

Table III: Fundamental Anisotropy Values in Propylene Glycol and Primol 342 of *n*-(9-Anthroyloxy) Fatty Acids

	excitation wavelength									
	316 nm			337 nm		353 nm		381 nm		
probe	PG −52[a]	PG −10[b]	PR +6[c]	PG −52[a]	PR +6[c]	PG −52[a]	PR +6[c]	PG −52[a]	PG −10[b]	PR +6[c]
2-AS	0.084	0.08	0.07	0.173	0.13	0.228	0.17	0.324	0.34	0.24
7-AS	0.089	0.09	0.08	0.178	0.15	0.233	0.20	0.324	0.33	0.26
9-AS	0.090	0.08	0.09	0.178	0.16	0.231	0.20	0.323	0.33	0.25
12-AS	0.088	0.08	0.08	0.177	0.16	0.230	0.22	0.322	0.33	0.25
16-AP	0.088	0.09	0.07	0.174	0.13	0.229	0.19	0.327	0.33	0.25

[a] Steady-state values in propylene glycol at −52 °C. [b] Zero-time values from anisotropy decay curves in propylene glycol at −10 °C. [c] Zero-time values from anisotropy decay curves in Primol 342 at 6 °C.

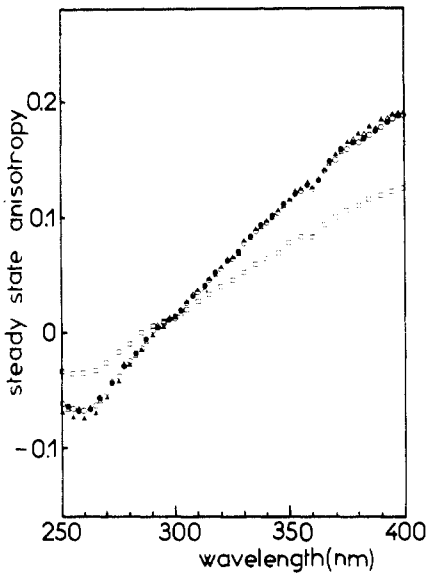

FIGURE 4: Anisotropy spectra of *n*-(9-anthroyloxy) fatty acids in Primol 342 at 6 °C: 2-AS (▲), 7-AS (○), 9-AS (●), 12-AS (△), and 16-AP (□). Probe concentration 7×10^{-5} M.

Table IV: Rotational Correlation Time Values (ns)[a] of the *n*-(9-Anthroyloxy) Fatty Acids in Primol 342 at 6 °C

	excitation wavelength[c]			
probe[b]	316 nm	337 nm	353 nm	381 nm
2-AS	18	21	27	31
7-AS	14	15	16	19
9-AS	13	14	14	18
12-AS	12	13	11	19
16-AP	9	11	9	9

[a] ±1 ns. [b] Probe concentration 1.5×10^{-5} M. [c] Band-pass 10, 2, 2, and 2 nm for 316, 337, 353, and 381 nm, respectively.

while those for the 16-AP are about 40% lower between 310 and 400 nm (Figure 4). Total intensity decay curves analysis reveals a single excited-state lifetime component for each probe (given below). The fundamental anisotropy values r_0 are not directly measurable in this medium, since a translucid gel state occurs at temperatures below −6 °C. Nevertheless, assuming the same value of r_0 for all probes (Tilley et al., 1979), it is possible to compare their average rotational rates. For the 7-, 9-, and 12-AS the same rotational rate can be deduced from identical values of r (Figure 4) and of the excited-state lifetimes [$\tau(\pm 0.2$ ns) = 10.6, 10.7, and 10.5 ns, respectively]. For 16-AP, a faster rotational motion can be inferred from the lower values of the anisotropy (Figure 4) and from the higher value of the excited-state lifetime ($\tau = 12.3 \pm 0.2$ ns). The excited-state lifetime value for 2-AS ($\tau = 12.6 \pm 0.2$ ns) is consistent with a lower rotational rate, since anisotropy plots for the 2-, 7-, 9-, and 12-AS are superimposable (Figure 4).

The rotational rate values of the probes measured by the time-resolved technique appear to be in the same increasing order (from the 2-AS to the 16-AP) (Table IV). All the experimental anisotropy decay curves were best fitted with one exponential term. For each probe, except for the 16-AP, increasing values of correlation time are observed with increasing excitation wavelength, i.e., with a larger contribution of the in-plane mode of rotation (Table IV). Therefore, it can be inferred that the in-plane correlation time is longer than the out-of-plane one. The values of $r_{t=0}$ obtained in Primol 342 at 6 °C are lower than those obtained in propylene glycol at −10 °C, especially at 381 nm (Table III). Therefore, experiments were performed with the 9-AS, using the synchrotron radiation available at the Orsay Linear Accelerator (1.7-ns flash duration), in order to resolve the anisotropy decay with higher accuracy. At 6 °C and 353 nm as excitation wavelength, a value of 0.195 is calculated for $r_{t=0}$ in good agreement with the corresponding value obtained in the laboratory (Table III). Another determination of the fundamental anisotropy values was also carried out at different excitation wavelengths according to the Perrin plot, giving extrapolated r_0 values equal to 0.075, 0.136, 0.179, and 0.242 for 316, 337, 353, and 381 nm, respectively (Figure 5). None of the fundamental anisotropy values obtained by these alternative methods reached the r_0 value measured in vitrified propylene glycol (Table III).

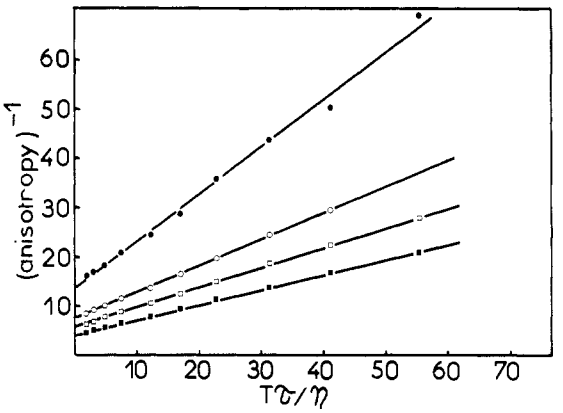

FIGURE 5: Perrin plots for the 9-AS in Primol 342. Temperature was varied from −5 to 40 °C, corresponding to excited-state lifetimes ranging from 10.5 to 9.7 ns. Excitation wavelength was selected at 316 (●), 337 (○), 353 (□), and 381 nm (■). Probe concentration 7×10^{-5} M.

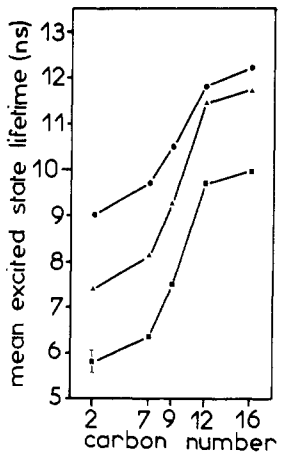

FIGURE 6: Mean excited-state lifetime values at 21 (●), 37 (▲), and 47 °C (■) for the *n*-(9-anthroyloxy) fatty acid derivatives in DPPC vesicles. The bar refers to the error in the decay time measurements and applies to all points.

Fluorescence Properties of n-(9-Anthroyloxy) Fatty Acids in Vesicles of DPPC. Time-resolved experiments were performed at three temperatures: at 21 and 37 °C, below the gel to liquid-crystalline transition, and at 47 °C, above this transition. In contrast to the results obtained in isotropic solvents, the total fluorescence intensity decays of all anthroyloxy fatty acid derivatives are fitted by a biexponential at each temperature. Both lifetimes are decreasing with increasing temperature (from 12 to 8 ns and 4 to 2 ns for the two components of 9-AS, for instance), but the weighting of the two time components is independent of temperature: 2/3 and 1/3 for the longer and shorter component, respectively. The mean excited-state lifetime values are given in Figure 6; they increase from the 2-AS to the 16-AP, the increase being sharper from 7-AS to 12-AS. The anisotropy measurements

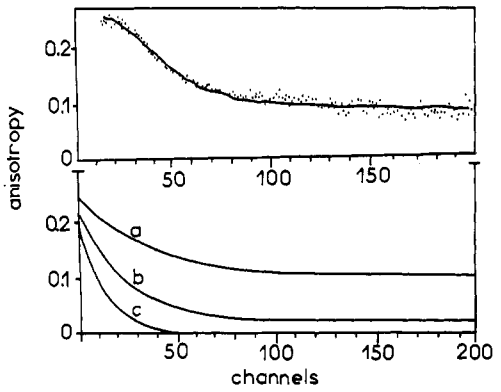

FIGURE 7: Anisotropy decays for the 9-AS in DPPC vesicles with excitation wavelength set at 381 nm (5-nm band-pass). (Upper part) Experimental (dots) and theoretical (solid lines) $d(t)/s(t)$ curves at 21 °C; (lower part) impulse anisotropy curves $r(t)$ at 21 (a), 37 (b), and 47 °C (c). Time resolution 0.217 ns/channel.

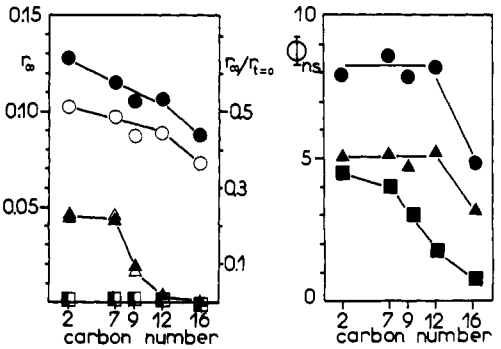

FIGURE 8: r_∞ and $r_\infty/r_{t=0}$ values (left part, filled and open symbols, respectively) and Φ (right part) values for the *n*-(9-anthroyloxy) fatty acid derivatives in DPPC vesicles. The excitation wavelength was set at 381 nm (5-nm band-pass); 21 (●), 37 (▲), and 47 °C (■).

indicate a rotational behavior of the probes different from the one observed in isotropic solvents.

At 381 nm as excitation wavelength, a nonzero asymptotic value of the anisotropy is observed below the transition temperature, as illustrated for 9-AS in Figure 7, and the anisotropy decays are represented by a single exponential term plus a constant $r(t) = (r_{t=0} - r_\infty)e^{-t/\phi} + r_\infty$. The results for all the probes are shown in Figure 8. At 21 °C, the values of r_∞ smoothly decrease from 0.13 to 0.09 for 2-AS to 16-AP, respectively. At 37 °C, the same r_∞ value of 0.05 is measured for the 2-AS and the 7-AS. This value decreases to 0.02 for the 9-AS and cancels out for the 12-AS and 16-AP. At 47 °C, r_∞ is equal to zero, whatever the probe (Figure 8, left part). The same figure (right part) shows the variations of ϕ. Below the transition, ϕ remains constant from the 2-AS to the 12-AS and decreases for 16-AP. In contrast, at 47 °C, where no hindrance is exerted on the motion of the probe, a continuous decrease of ϕ is observed from the 2-AS to the 16-AP. The $r_{t=0}$ values are lower that those obtained in propylene glycol at −52 °C. Moreover, a significant diminution of $r_{t=0}$ values is observed with increasing temperature, these values being the same for all probes at each temperature (Table V). The $r_\infty/r_{t=0}$ ratios, which afford a quantitative evaluation of the hindrances, are plotted in Figure 8 (left part).

At 316 nm as excitation wavelength, the observed rotations are unhindered for all probes whatever the temperature, as illustrated for 9-AS in Figure 9; all the anisotropy decays are represented by a monoexponential term. The variations of the correlation times ϕ at 21 and 37 °C are given in Figure 10. At 47 °C, the rotations were too fast and prevented precise measurements. At this wavelength the $r_{t=0}$ values are close

Table V: Zero-Time Anisotropy Values Computed from Anisotropy Decay for *n*-(9-Anthroyloxy) Fatty Acids in DPPC Vesicles

	excitation wavelength				
	316 nm at temp (°C)		381 nm at temp (°C)		
probe	21	37	21	37	47
2-AS	0.080	0.075	0.250	0.210	0.183
7-AS	0.075	0.091	0.244	0.225	0.183
9-AS	0.082	0.094	0.246	0.210	0.186
12-AS	0.076	0.076	0.253	0.183	0.203
16-AP	0.070	0.091	0.233	0.170	0.206

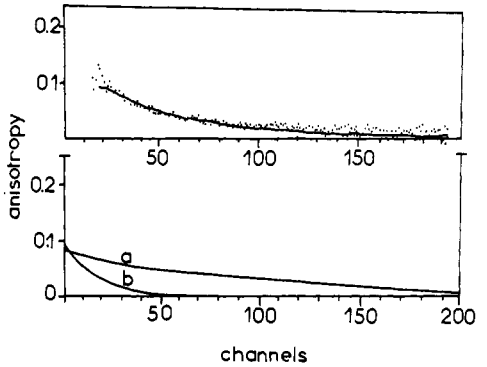

FIGURE 9: Anisotropy decays for the 9-AS in DPPC vesicles with excitation wavelength set at 316 nm (10-nm band-pass). (Upper part) Experimental (dots) and theoretical (solid lines) $d(t)/s(t)$ curves at 21 °C; (lower part) impulse anisotropy curves $r(t)$ at 21 (a) and 37 °C (b). Time resolution 0.217 ns/channel.

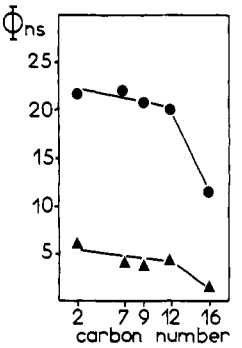

FIGURE 10: Φ values for the set of *n*-(9-anthroyloxy) fatty acids in DPPC vesicles. Excitation wavelength 316 nm (10-nm band-pass); 21 (●) and 37 °C (▲).

to the fundamental anisotropy values obtained in propylene glycol (Table V).

Discussion

Interpretation of the Depolarizing Rotations of the Probes. For most of the planar aromatic fluorophores which have been studied up to now, including anthracene derivatives, absorption and emission oscillators are contained in the plane of the molecule (Birks, 1970; Berlman, 1971). Their motional properties can be characterized by two modes of rotation: in-plane and out-of-plane (Shinitzky et al., 1971; Valeur & Weber, 1978; Lakowicz & Knutson, 1980). For the *n*-(9-anthroyloxy) fatty acids, which have been used as fluorescent probes in the present study, the question arises as to the direction of the out-of-plane axis of rotation relative to the symmetry axes of the anthroyl ring and to the acyl chain. If an absorption oscillator along the short axis is assumed as for anthracene (Badley et al., 1973), the out-of-plane motion observed for small rotations should occur around the long axis (Weber, 1971). However, the r_0 values measured in the

long-wavelength band (300–400 nm) exhibit continuous changes. Such behavior can be related to the observations of Williams (1957) who reported that inductive substituents on C-9 or C-10 of the anthracene ring strikingly enhance a weak absorption transition (long-axis oriented) which lies under the stronger transition at long wavelengths. This enhancement would be associated to a lowering of the r_0 values in the short-wavelength range below the values measured for unsubstituted anthracene (Williams, 1957). Such lowering is actually observed for the r_0 values of the *n*-(9-anthroyloxy) fatty acids (Figure 1) as compared to the values reported for anthracene (Valeur & Weber, 1978). Therefore, by taking into account the presence of this long-axis oriented absorption transition, the out-of-plane motion around the short axis of the anthroyl ring would also contribute to the depolarizing rotations of these probes. From steady-state measurements at different excitation wavelengths or from time-resolved analysis at 316 nm, only one out-of-plane rotational rate is evidenced in isotropic solvents. Moreover, the two rates of rotational motion (in-plane and out-of-plane) are of the same order of magnitude for each probe. Thus, in the fluorescence time scale, the rotating unit behaves as an approximate symetric rotor, differing from anthracene which can be considered as an asymetric rotor (Mantulin & Weber, 1977; Valeur & Weber, 1978). This different behavior could be assigned to the substitution on the anthroyl ring by the fatty acid. Furthermore, Johns et al. (1979) have suggested from ^{13}C NMR studies of the same probes that the anthroyl ring and the carbon atom on which it is attached move as one unit. This would explain the slowing down of the in-plane motion with respect to the out-of-plane one. The out-of-plane rotations would occur relatively freely around the ester linkage, whereas the in-plane motion would be more dependent on the acyl chain reorientation.

Study of the Probes in Isotropic Solvents. In propylene glycol, though the correlation time values given by the steady-state measurements are higher than those given by the time-resolved analysis, a good agreement is obtained for the comparison between the different probes: the 2-, 7-, 9-, and 12-AS behave in a rather similar way while the 16-AP appears to rotate faster than the other probes. This could be assigned to the particular substitution location of the fluorophore in the 16-AP, i.e., at the end of the fatty acid chain.

In Primol 342, both 2-AS and 16-AP rotational motions are different from those of 7-, 9-, and 12-AS. The lower rate of rotation of 2-AS as compared to those of 7-, 9-, and 12-AS is consistent with the existence of a hydrogen bond between the carboxylic group of the fatty acid and the anthroyl ring (Werner & Hercules, 1969), retarding the fluorophore motion. Such slowing down of the motion of the 2-AS as compared to the other derivatives has also been observed by steady-state measurements in another paraffinic oil (Tilley et al., 1979). Since no such difference has been observed for the 2-AS in propylene glycol, this may be characteristic of the effects of nonprotic solvents.

In experimental conditions where both solvents have the same bulk viscosity, the systematic higher rate values found for each probe in Primol 342 as compared to propylene glycol can be attributed to a lower solvation of the fluorophore by the former solvent, leading to a smaller rotating unit.

Study of the Probes in DPPC Vesicles. The fluorescence properties of the fatty acid derivatives have been examined in DPPC vesicles which undergo two thermal transitions. The studies have been performed at three temperatures corresponding to different lipid phases: at 21, 37, and 47 °C corresponding respectively to the $L_{\beta'}$, $P_{\beta'}$, and L_α phases (Janiak et al., 1976).

In all other reported fluorescence time-resolved studies in lipid systems, hindered rotations have been evidenced whatever the probe (Kawato et al., 1977; Badea et al., 1978; Wolber & Hudson, 1981; Chen et al., 1977; Wahl et al., 1971; Lakowicz & Knutson, 1980). In contrast, one of the important results of this study is the existence of an unhindered motion of the fluorophore. Such unhindered motion is observed when excitation wavelength is set at 316 nm and therefore can be assigned to the out-of-plane rotation of the anthroyl ring. This rotation, which would mainly occur around the ester linkage (nearly perpendicular to the hydrocarbon chain) as discussed above, should be affected only by the frictional forces exerted by the phospholipid acyl chains. On the other hand, when both in-plane and out-of-plane motions contribute to the depolarizing rotations, a motional hindrance is evidenced by the existence of an r_∞ value in the anisotropy decay. Therefore, the r_∞ value is a characteristic of the in-plane mode of rotation and would reflect the hindrances exerted by the phospholipid organization on the reorientational motion of the fatty acid chain.

At 21 °C ($L_{\beta'}$ gel phase), the $r_\infty/r_{t=0}$ ratios obtained at 381 nm evidence a slight variation of the degree of orientational constraint as a function of the labeled depth (Figure 9). At this wavelength, the ϕ values reflect both hindered (in-plane) and unhindered (out-of-plane) motions, and the delineation of the respective components is not possible in the present experimental conditions. Only the ϕ value for the 16-AP differs from those obtained for the other probes, a result which could be related to the particular motional behavior of this probe in isotropic solvents. At 316 nm, where only the unhindered out-of-plane motion is observed, ϕ is an effective correlation time and reflects the fluidity at different levels of the bilayer. Since the variation of ϕ, as a function of the substitution position of the fluorophore, parallels the one observed in isotropic solvent, a uniform fluidity with increasing depths can be deduced.

At 37 °C ($P_{\beta'}$ gel phase) and with an excitation wavelength of 381 nm, the significant drop of the $r_\infty/r_{t=0}$ ratio for 12-AS and 16-AP as compared to the 2-AS (Figure 8) argues in favor of lipid structural changes mainly localized in the hydrophobic core of the bilayer. This is consistent with the results of Lentz et al. (1978) and Levin & Fowler Bush (1981), although the chemical nature of the polar head groups was shown to be essential for the existence of the pretransition (Ladbrooke & Chapman, 1969; Vaughan & Keough, 1974; Janiak et al., 1976). At 381 nm, the variation of ϕ as a function of the carbon substitution is similar to the one at 21 °C, all values being smaller. The ϕ values measured at 316 nm indicate a large enhancement of the fluidity as compared to the $L_{\beta'}$ gel phase, whatever the membrane level.

At 47 °C (L_α liquid-crystalline phase), and with 381 nm as excitation wavelength, the anisotropy decays are asymptotic to zero whatever the membrane depth. This is in contrast with the results obtained with all other probes in similar systems and especially with DPH, for which the persistence of a nonzero value of the anisotropy is observed above the lipid transition temperature (Chen et al., 1977; Kawato et al., 1977). This may result from a different orientation of the emission oscillator for DPH and the anthroyl ring [respectively perpendicular (Andrich & Vanderkooi, 1974) and parallel to the membrane plane (Badley et al., 1973)]. With the same excitation wavelength (381 nm) a steep fluidity gradient in the bilayer can be inferred from the correlation time variations,

since no similar changes are observed in isotropic solvents.

The divergence between the $r_{t=0}$ values obtained in hydrophobic media (DPPC vesicles and Primol 342) as compared to those obtained in vitrified propylene glycol raises some questions. The good agreement found between the data obtained from steady-state measurements in propylene glycol at −52 °C and those issued from anisotropy decays in the same medium at −10 °C is good evidence for the effectiveness of our nanosecond apparatus and our numerical fitting procedures. Furthermore, similar $r_{t=0}$ values are obtained in Primol 342 with either our nanosecond apparatus or a shorter flash excitation from the synchrotron radiation, in agreement with the extrapolated r_0 values obtained from the Perrin plot. Therefore, one explanation of the divergence observed would be the existence of a very short time component in the anisotropy decay (Wahl et al., 1971) in Primol 342 and DPPC vesicles, in agreement with the temperature dependence observed in the latter system. An alternative explanation could involve a fast torsional vibration process of the excited state occurring in a very short time period (Jablonski, 1960, 1965).

In conclusion, both hindered and unhindered rotations were evidenced for the *n*-(9-anthroyloxy) fatty acids embedded in DPPC vesicles, depending on the experimental observation conditions. By selecting a suitable excitation wavelength, the out-of-plane rate of rotation of the fluorophore was separately monitored, and we have shown that no hindrance is exerted on this type of motion. On the other hand, the hindered depolarizing rotations could be specifically attributed to the in-plane motion. These results allow the determination of different parameters characteristic of the membrane. Monitoring the out-of-plane mode of rotation, an evaluation of a fluidity gradient is allowed either by the time-resolved or by the steady-state technique since the zero value of the limiting anisotropy r_∞ has no effect on the computation of the rotational correlation times. For this evaluation one has to take into account the intrinsic motional properties of the fluorophore as a function of its substitution position on the fatty acid chain.

For excitation wavelengths where a nonzero value of r_∞ is observed, the time-resolved technique brings information about the lipid organization at different depths through the bilayer leaflet.

Acknowledgments

We thank J. C. Brochon (Laboratoire pour l'Utilisation du Rayonnement Electromagnétique, Orsay, France) for making available the short excitation flash from the synchrotron radiation. We are grateful to L. Lewis for careful correction of the English.

References

Andrich, M. P., & Vanderkooi, J. M. (1976) *Biochemistry 15*, 1257–1261.

Badea, M. G., de Toma, R. P., & Brand, L. (1978) *Biophys. J. 24*, 197–212.

Badley, R. A., Martin, W. G., & Schneider, H. (1973) *Biochemistry 12*, 268–275.

Berlman, I. B. (1971) *Handbook of Fluorescence Spectra of Aromatic Molecules*, pp 78–79, Academic Press, New York.

Birks, J. B. (1970) *Photophysics of Aromatic Molecules*, p 7, Wiley-Interscience, London.

Chen, L. A., Dale, R. E., Roth, S., & Brand, L. (1977) *J. Biol. Chem. 252*, 2163–2169.

Dale, R. E., Chen, L. A., & Brand, L. (1977) *J. Biol. Chem. 252*, 7500–7510.

de Paillerets, C., Gallay, J., Vincent, M., & Alfsen, A. (1981) *Biochim. Biophys. Acta 664*, 134–142.

Gallay, J., Vincent, M., de Paillerets, C., Rogard, M., & Alfsen, A. (1981) *J. Biol. Chem. 256*, 1235–1241.

Haigh, E. A., Thulborn, K. R., & Sawyer, W. H. (1979) *Biochemistry 18*, 3525–3532.

Hare, F., & Lussan, C. (1977) *Biochim. Biophys. Acta 467*, 262–272.

Hare, F., Amiel, J., & Lussan, C. (1979) *Biochim. Biophys. Acta 555*, 388–408.

Heyn, M. P. (1979) *FEBS Lett. 108*, 359–364.

Jablonski, A. (1960) *Bull. Acad. Pol. Sci., Ser. Sci., Math., Astron. Phys. 8*, 655–660.

Jablonski, A. (1965) *Acta Phys. Pol. 28*, 717–728.

Janiak, M. J., Small, D. M., & Shipley, G. G. (1976) *Biochemistry 15*, 4575–4580.

Johns, S. R., Willing, R. I., Thulborn, K. R., & Sawyer, W. H. (1979) *Chem. Phys. Lipids 24*, 11–16.

Kawato, S., Kinosita, K., & Ikegami, A. (1977) *Biochemistry 16*, 2319–2324.

Kinosita, K., Mitaku, S., Ikegami, A., Ohbo, N., & Kunii, T. L. (1976) *Jpn. J. Appl. Phys. 15*, 2433–2440.

Kinosita, K., Kawato, S., & Ikegami, A. (1977) *Biophys. J. 20*, 289–305.

Kremer, J. M. H., Esker, M. W., Pathmamanoharan, C., & Wiersema, P. H. (1977) *Biochemistry 16*, 3932–3935.

Ladbrooke, B. D., & Chapman, D. (1969) *Chem. Phys. Lipids 3*, 304–367.

Lakowicz, J. R., & Knutson, J. R. (1980) *Biochemistry 19*, 905–911.

Lakowicz, J. R., Prendergast, F. G., & Hogen, D. (1979) *Biochemistry 18*, 520–527.

Lentz, B. R., Barenholz, Y., & Thompson, T. E. (1976) *Biochemistry 15*, 4521–4528.

Lentz, B. R., Freire, E., & Biltonen, R. L. (1978) *Biochemistry 17*, 4475–4480.

Levin, I. W., & Fowler Bush, S. F. (1981) *Biochim. Biophys. Acta 640*, 760–766.

Lipari, G., & Szabo, A. (1980) *Biophys. J. 30*, 489–506.

Mantulin, W. W., & Weber, G. (1977) *J. Chem. Phys. 66*, 4092–4099.

Perrin, F. (1926) *J. Phys. Radium 7*, 390–401.

Perrin, F. (1936) *J. Phys. Radium 7*, 1–11.

Shinitzky, M., & Barenholtz, Y. (1978) *Biochim. Biophys. Acta 515*, 367–394.

Shinitzky, M., Dianoux, A. C., Gitler, C., & Weber, G. (1971) *Biochemistry 10*, 2106–2113.

Thulborn, K. R., & Sawyer, W. H. (1978) *Biochim. Biophys. Acta 511*, 125–140.

Tilley, L., Thulborn, K. R., & Sawyer, W. H. (1979) *J. Biol. Chem. 254*, 2592–2594.

Valeur, B. (1978) *Chem. Phys. 30*, 1–11.

Valeur, B., & Weber, G. (1978) *J. Chem. Phys. 69*, 2393–2400.

Vanderkooi, J., & McLaughlin, A. (1975) in *Biochemical Fluorescence Concepts* (Chen, R. F., & Edelhoch, H., Eds.) Vol. 2, Chapter 19, Marcel Dekker, New York.

Vanderkooi, J., Fischkoff, S., Chance, B., & Cooper, R. A. (1974) *Biochemistry 13*, 1589–1595.

Vaughan, D. J., & Keough, K. M. (1974) *FEBS Lett. 47*, 158–161.

Wahl, P. (1975a) *Chem. Phys. 7*, 210–219.

Wahl, P. (1975b) *Chem. Phys. 7*, 220–228.

Wahl, P., Kasai, M., & Changeux, J. P. (1971) *Eur. J. Biochem. 18*, 332–341.

Weber, G. (1953) *Adv. Protein Chem. 8*, 415–459.

Weber, G. (1971) J. Chem. Phys. 55, 2399-2407.
Werner, T. C., & Hercules, D. M. (1969) J. Phys. Chem. 73, 2005-2011.
Williams, R. (1957) J. Chem. Phys. 26, 1186-1188.
Wolber, P. K., & Hudson, B. S. (1981) Biochemistry 20, 2800-2810.
Yguerabide, J., Epstein, H. F., & Stryer, L. (1970) J. Mol. Biol. 51, 573-590.

Purification, Composition, and Physical Properties of a Thermal Hysteresis "Antifreeze" Protein from Larvae of the Beetle, *Tenebrio molitor*†

A. P. Tomchaney, J. P. Morris, S. H. Kang, and J. G. Duman*

ABSTRACT: Proteins which produce a thermal hysteresis (difference between the freezing and melting points) in aqueous solution are well-known for their antifreeze activity in polar marine fishes. Much less is known about the biology and biochemistry of similar antifreeze proteins found in certain insects. A thermal hysteresis protein was purified from cold acclimated larvae of the beetle, *Tenebrio molitor*, by using ethanol fractionation, DEAE ion-exchange chromatography, gel filtration, and high-pressure liquid chromatography. The purified protein had a molecular mass of 17 000 daltons and its N terminus was lysine. The amino acid composition of the antifreeze protein contained more hydrophilic amino acids than the fish antifreezes. This is consistent with the compositions of previously purified insect thermal hysteresis proteins. However, the percentage of hydrophilic amino acids in this *Tenebrio* antifreeze protein was considerably less than that of other insect thermal hysteresis proteins. The freezing point depressing activity of the *Tenebrio* antifreeze was less than that of fish proteins and glycoproteins at low protein concentrations but was greater at high protein concentrations.

Several species of overwintering insects are now known to produce proteinaceous antifreezes which significantly lower both the freezing and supercooling points of the insects' body fluids (Duman, 1977a,b, 1980; Patterson & Duman, 1978, 1981). These proteins produce a thermal hysteresis whereby the freezing point of an aqueous solution containing the protein is depressed, by a noncolligative mechanism, well below the melting point of the solution. This behavior is quite similar to that caused by the protein and glycoprotein antifreezes used by polar marine fishes (DeVries, 1980; Yeh & Feeney, 1978). The unique, repeating primary structure of the fish antifreezes (DeVries, 1971; DeVries & Lin, 1977) combined with their higher order structure allows the proteins to hydrogen bond (via the hydrophilic amino acid side chains in the case of the proteins and by means of the hydroxyl groups of the carbohydrates in the case of the glycoproteins) to the ice lattice and thereby "poison" any possible seed ice crystals which might be present in the system (Raymond & DeVries, 1977; DeVries & Lin, 1977). This effectively lowers the freezing point of the solution while not significantly changing the melting point. It is likely that the insect thermal hysteresis proteins (THP's) operate by the same mechanism. It is also possible that the THP's promote supercooling by a similar mechanism. As the temperature of an aqueous solution is lowered below its freezing point, in the absence of a seed crystal, water molecules form into small icelike clusters called embryo crystals. These may form spontaneously or they may form around various heterogeneous nuclei. These embryo crystals form, break up, and re-form. As the temperature is lowered, the size of the embryo crystals increases until a critical radius is reached and the embryo crystal seeds the solution (Knight, 1967). It is quite possible that the THP's may bind to the surface of embryo crystals and/or heterogeneous nuclei and thereby promote supercooling by inhibiting the growth of embryo crystals.

Insect THP's have not been as extensively investigated as have those of the fishes; however, THP's have been purified from two insect species—the milkeweed bug, *Oncopeltus fasciatus* (Patterson et al., 1981), and the larvae of the Tenebrionid beetle, *Tenebrio molitor* (Patterson & Duman, 1979; Schneppenheim & Theede, 1980). The insect THP's in general are composed of considerably more hydrophilic amino acids and lack the large percentage of alanine found in most of the fish THP's (generally over 60% of the amino acid residues). *T. molitor* is quite unusual in that it produces a number of THP's which differ significantly in amino acid composition. The purpose of this paper is to present the purification, composition, and properties of a *Tenebrio* THP which has not been previously reported.

Experimental Procedures

Materials. *T. molitor* cultures were purchased from Carolina Biological Supply. DEAE-Sephadex and Sephadex G-100 were purchased from Pharmacia. Spectrapor dialysis tubing was from Fisher Scientific. All electrophoresis materials (acrylamide, *N,N'*-methylenebis(acrylamide), sodium dodecyl sulfate, ammonium persulfate, glycine, *N,N,N',N'*-tetramethylethylenediamine, Coomassie blue, and molecular weight standards) were purchased from Bio-Rad Laboratories. The standard phenylthiohydantoin derivatives of the amino acids and the polyamide thin-layer chromatography sheets used in the N-terminal analysis were from the Pierce Chemical Co.

Acclimation. *Tenebrio* larvae were acclimated to low temperatures and a short photoperiod to induce THP production (Patterson & Duman, 1978). Larvae were held for 1 week in a Precision Scientific Model 805 incubator at a photoperiod

† From the Department of Biology (A.P.T., S.H.K., and J.G.D.) and Department of Chemistry (J.P.M.), University of Notre Dame, Notre Dame, Indiana 46556. *Received September 4, 1981.* This work was supported by National Science Foundation Grant No. PCM77-03475 to J.G.D. J.P.M. was supported by Grant HL-13423 from the National Institutes of Health. S.H.K. is supported by National Institutes of Health Grant No. AI 10707 to M. S. Fuchs and S.H.K.

0006-2960/82/0421-0716$01.25/0